# Engineering Flowfield Method with Angle-of-Attack Applications

E. V. Zoby* and A. L. Simmonds †
*NASA Langley Research Center, Hampton, Virginia*

**An approximate inviscid flowfield method has been extended to include heat-transfer predictions and a technique to account for the effect of variable-entropy edge conditions on the heat transfer. Results of the approximate code have been validated by comparison with experimental data and results of detailed predictions. The engineering code computes the inviscid flowfield and convective heating over hyperboloids, ellipsoids, paraboloids, and sphere-cones at zero deg angle of attack (AOA). An application to angle-of-attack conditions is included in the present method by using existing approximations to: 1) account for the streamline-spreading effects on the heat transfer along the windward and leeward rays of sphere-cones and 2) to compute the corresponding circumferential heating. Present results of the engineering calculations are shown to be in good agreement with existing pressure and heating data over sphere-cones, even at high incidence values, with the restriction that the sonic-line location remain on the spherical cap. The present technique has been demonstrated to provide a rapid but reliable method for predicting surface-measurable quantities and flow properties through the shock layer. The code represents a versatile engineering method for parametric or preliminary thermal design studies.**

## Nomenclature

$H$ = enthalpy
$H_2$ = Streamline-spreading metric
$h$ = heat-transfer coefficient
$L$ = body length
$L_q$ = leeward heating-rate ratio, $q_\alpha/q_{\alpha=0}$
$M$ = Mach number
$N$ = reciprocal exponent in velocity profile power law
$p$ = pressure
$\dot{q}$ = heating rate
$R$ = radius of curvature
$R_\theta$ = momentum thickness Reynolds number
$r$ = cross-sectional radius
$S$ = surface-wetted distance
$u$ = tangential velocity
$v$ = normal velocity
$W_q$ = windward heating-rate ratio, $q_\alpha/q_{\alpha=0}$
$w$ = effective cone half angle, Eq. (10)
$x$ = shock arc length
$z$ = axial length
$\alpha$ = angle of attack
$\gamma$ = specific heat ratio
$\phi$ = meridian ray
$\psi$ = stream function
$\sigma_{st}$ = second derivative of stagnation-point shock radius of curvature
$\theta$ = momentum thickness
$\theta_c$ = cone half-angle
$\theta_s$ = local shock angle
$\theta_{sc}$ = sharp cone shock angle

*Subscripts*

$\alpha$ = angle of attack
$\infty$ = freestream
$n$ = nose radius
$s$ = shock
$st$ = stagnation condition
$w$ = wall condition

Presented as Paper 84-0303 at the AIAA 22nd Aerospace Sciences Meeting, Reno, Nev., Jan. 9-12, 1984; submitted Feb. 7, 1984; revision received July 9, 1984. This paper is declared a work of the U.S. Government and therefore is in the public domain.

*Aero-Space Technologist, Aerothermodynamics Branch, Space Systems Divison. Member AIAA.
†Mathematician, Aerothermodynamics Branch, Space Systems Division. Member AIAA.

## Introduction

APPROXIMATE convective heating techniques[1-16] which have been substantiated by experimental data[17-24] and/or "benchmark" calculations[25-33] are employed frequently in parametric or design calculations for most ballistic and maneuvering reentry spacecraft. The approximate codes are of practical importance, since the detailed codes typically require large computer run times and storage. However, these approximate methods are typically limited in application to either a particular gas composition, stagnation-point solution, perfect gas analysis, or constant entropy solution. None of the above noted approximate techniques provide the flexibility of determining flow property distributions through the shock layer. For these approximate methods to have a wide range of applicability (outer planet missions and Earth space transportation systems) they should be capable of modeling a variety of flow phenomena such as arbitrary reactive-gas compositions and variable-entropy effects, as well as a wide range of body geometries.

A recent investigation[34] proposed approximate laminar and turbulent heating techniques for use in nonreacting and equilibrium hypersonic flow calculations. The heating methods were coupled with inviscid flowfield codes [35,36] to provide procedures for evaluating the impact of variable-entropy conditions on the surface heating. The coupling of the approximate flowfield code[36] with the heating methods constituted an engineering code which has been used in aerothermal studies at Earth, Venusian, and outerplanet entry conditions. In addition to calculation of the heat-transfer and pressure distribution, the code provides detailed distributions of flowfield properties which are not available in typical engineering heating analyses. Heat-transfer results based on the approximate code were shown to be in good agreement with a range of ground-test data and with predictions based on detailed codes. Recently, heat-transfer predictions based on the engineering code and using an "equivalent" axisymmetric body concept to define the shuttle windward-

ray geometry were shown to be in good agreement with Shuttle ground test[37] and free-flight[38] experimental heating rates. However, this engineering code is an axisymmetric zero angle-of-attack code with analytic expressions for bow shocks capable of generating body shapes closely approximating only hyperboloids or spherically blunted cones. In addition, due to an assumption of a constant sharp-cone shock angle along the sphere-cone frustum, inviscid flowfield solutions for half-cone angles less than approximately 25 deg cannot be computed.

The purpose of this paper is to present the results of an investigation initiated to develop a more flexible engineering code. The approach is to couple the heating and the constant or variable-entropy edge assumptions, based on perfect or equilibrium gas calculations with a different approximate inviscid code.[39] The engineering code used in this investigation (inviscid plus heating and entropy methods) has the capability to compute the inviscid flowfield and heating distributions for a range of analytic shapes, i.e., paraboloids, hyperboloids, and ellipsoids, as well as moderately blunt (supersonic flow along flank) or slender sphere-cones at zero angle of attack (AOA). The inviscid code assumes an initial bow shock which is iterated until convergence of computed and desired body is obtained. The current engineering code is validated with the same data as the original code. For sphere-cones at incidence, existing approximations which account for the effect of streamline spreading[16] on the windward and leeward convective heat-transfer rates and which provide procedures to compute meridian pressure distributions and the peripheral heat-flux distributions[40] are also incorporated in the present method. In this paper, capabilities of the present engineering code are demonstrated by comparing predictions with experimental pressure and heat-transfer data over slender blunt cones at incidence. The necessity of including an approximation for the streamline metric $H_2$ (a measure of streamline spreading) in the heating calculations compared to using only the equivalent-cone method is noted.

## Analysis

In this section, several important aspects of the present engineering method are reviewed: the assumptions and basic equations of the approximate inviscid code,[39] the flow options, the laminar and turbulent heating equations, and the procedures to account for streamline-spreading effects on the windward and leeward symmetry plane heat transfer to compute the circumferential heating distributions and meridional pressure distributions over cones at incidence levels for which the sonic-line location remains on the spherical cap.

### Inviscid Code

An approximate inviscid code[39] based on the Maslen[41] technique is used in the analysis to compute the zero AOA flowfield over paraboloids, ellipsoids, hyperboloids, and sphere-cones. There is an important difference in the present inviscid technique[39] compared to the initial inviscid method[36] that was used in previous aerothermal analyses. The previous inviscid method employed analytic expressions for the shock that resulted in only closely approximating the desired body. The present solution techniques assumes an initial bow shock wave which is iterated until satisfactory convergence with the desired body is obtained. The inviscid method has been presented in detail and only a brief description is given herein.

Maslen applies the Von Mises transformation to the governing equations so that the independent variables are the distance along the shock, $x$, and the stream function, $\psi$. Calculations proceed along rays normal to the shock. The calculation procedure is significantly simplified based on an assumption by Maslen that the streamlines for hypersonic flow are nearly parallel to the shock. The assumption leads to the determination of an explicit algebraic expression for the normal pressure distribution through the shock layer. In a later investigation,[42] Maslen presents another approximation to account for the contribution of the normal velocity component through the shock layer to the pressure level. The pressure equation is

$$p(\psi) = P_s + \frac{u_s}{r_s R_s} - (\psi - \psi_s) - \frac{v_s \tan\theta_s}{r_s}\left(\frac{1}{R_s} + \frac{\cos\theta_s}{r_s}\right)\frac{\psi^2 - \psi_s^2}{2\psi_s} \tag{1}$$

Calculated results based in Eq. (1), in contrast to calculated results based on the first pressure relation,[41] yield improved comparisons[39] with detailed predictions of the surface pressure. Note that with Eq. (1), an approximate expression for the normal velocity component was included in the energy equation in the present method.

The iterative flowfield method, which was initially discussed in Ref. 43 and later modified,[39] is divided into two regions, subsonic and supersonic. For the region referred to as the subsonic region, the shock shape is represented by a Taylor series as

$$R_s(x) = R_{s,st} + \sigma_{st}\frac{x_s^2}{2} \tag{2}$$

The shock shape is computed to an arc length location defined by a shock Mach number of approximately 1.3 or 1.7 for perfect gas or equilibrium chemistry conditions, respectively. This requirement ensures a continually increasing shock radius of curvature between the subsonic and supersonic regions. The local flow properties and geometry are computed until the body ($\psi = 0$) is reached. The computed body is scaled to the desired body and the scaling yields a new shock-shape definition. The process is repeated until the computed and desired body locations are within a specified convergence criterion. In the supersonic regions, a step-by-step marching procedure is used to compute the shock shape and flowfield. The same equations used in the subsonic region for the calculation of the flowfield properties and geometry are applicable. On subsequent iterations the increment in the shock radius of curvature is varied until satisfactory convergence is obtained. The shock arc length is held constant for the iteration process in the supersonic region. For sphere-cone solutions, additional analysis is required. The shock arc length is held constant, rather than the shock angle during iterations in the supersonic region, since the sphere-cone minimum shock-inflection point was found easier to compute. However, a present procedure different than the version in Ref. 39 is used for computing the flowfield downstream of the sphere-cone shock inflection point. This approach, which is based on related sharp cone techniques and yields improved predictions of surface pressures and heat transfer, is used since it is difficult to obtain satisfactory convergence by applying the upstream solution techniques to the nearly constant shock angle and relatively large values for the shock radius of curvature that are typical of this flowfield region of sphere-cones.

### Flow Options

In addition to the range of axisymmetric geometries, the code provides additional options for computing the flowfield solutions. Inviscid flowfield or inviscid plus heating solutions can be computed for perfect gas or equilibrium chemistry conditions. Eqilibrium gas calculations for air, $C0_2$-$N_2$, $H_2$-He and $CF_4$ gas mixtures are based on correlation equations for the enthalpy and temperature in terms of pressure-density relations. The flow properties used in the heating methods are based on either constant or variable-entropy edge conditions.

### Heat-Transfer Methods

Laminar and turbulent heating methods appropriate for engineering predictions of the convective heating rates about

reentry spacecraft at hypersonic flow conditions have been reported.[34] These approximate techniques were determined initially for outer-planet entry conditions, but are general in nature and can be applied to both perfect gas and equilibrium gas mixtures, i.e., no constants are adjusted for different gases and for either constant or variable entropy edge conditions. The results of the present heat-transfer predictions have been shown to be generally within 10% of experimental data or results of detailed prediction methods for Earth, Venusian, or outer-planet entry conditions. The set of equations for heating and variable-entropy edge conditions has been reported[34] in detail and only a brief discussion is presented herein.

*Background*

For both the stagnation-point heating rate and laminar heat-transfer distribution, results based on several analyses[1-4] are in good agreement, but the analyses are restricted to air. For gas compositions other than air, approximate methods are also available.[5,6] The analysis of Sutton and Graves,[5] while limited to the stagnation point of a blunt body, provides a versatile technique of calculating the stagnation-point heat-transfer rate in a wide range of base gases and in mixtures of these gases. The analysis of Marvin and Deiwert[6] provides a method of calculating the laminar-heating distribution, but for only a limited number of gas mixtures.

Approximate turbulent heat-transfer expression,[7-12] are primarily based on equating the skin friction to the Stanton number through the Reynolds analogy. In Refs. 8-11, the skin-friction relation as a function of the momentum thickness Reynolds number ($R_\theta$) is determined by assuming a velocity profile $[u/u_e = (Y/\delta)^{1/N}]$ to compute the required constants and exponents. For these references, a 1/7 power-law velocity profile is assumed. Differences in the skin-friction equations are due to either the form of the compressible transformations or the value of the form factor. In Ref. 12, the Spalding-Chi[44] skin-friction relation is used. The Spalding-Chi method has been shown[45] to yield good comparison with experimental ground-test data for heat transfer and skin friction over a wide range of test conditions. However, it has been shown that the method does not produce the best comparison with flight data.[7]

*Selected Method*

The technique of Sutton and Graves[5] is used for the calculation of the stagnation point heat-transfer rate, since the method can be applied by a simple but accurate procedure to a wide range of gas mixtures.

For the calculation of the laminar heat-transfer distribution, a method similar to those presented in Refs. 2-4 and 6 are not available for application to a wide range of gas mixtures. Thus, the laminar distributions are computed herein by relating heat transfer to a skin-friction relation based on $R_\theta$ through a modified Reynolds analogy form. This approach has a twofold purpose since a momentum or boundary-layer thickness is used in the method for approximating the variable-entropy effects on the heat-transfer calculations.

The turbulent heat transfer is also computed by using a skin-friction coefficient based on $R_\theta$. Published results[8-11] using this form for the skin-friction relation assume a 1/7th power velocity profile, but it has been noted[46,47] that the 1/7th power profile is not applicable over an extensive Reynolds number range. Axisymmetric nozzle wall data[48] which show $N$ to be a function of $R_\theta$ with values of $N$ as low as 4 for $R_\theta$ equal to approximately 1000 have been curve fit in terms of $R_\theta$. The subsequent expressions for the turbulent heat-transfer rate and momentum thickness reflect the dependence on $N$.

**Local Conditions**

Heat-transfer calculations, based on integral or detailed boundary-layer techniques, require inviscid properties external to the boundary layer. Usually, the external flow is assumed to be at a constant-entropy condition corresponding either to the oblique-shock or stagnation-point entropy. In general, however, the assumption of a constant-entropy value does not provide an adequate description of the external flow properties over the entire length of a blunt body in high-speed flow. This situation is caused by the highly curved shocks produced by blunt bodies. These shocks generate entropy gradients in the inviscid flow, resulting in inviscid tangential velocity gradients normal to the body surface.[49] Streamlines of varying entropy value, which pass through different points on the shock, are gradually embedded in the boundary layer as it grows along the surface. This process is referred to as streamline swallowing.

There are at least two techniques which account for the effect of variable-entropy flows on the surface heat and skin friction. One method is with the Viscous-Shock-Layer (VSL)[32,33] or Parabolized Navier-Stokes (PNS)[30,31] codes, which provided a direct means of accounting for the entropy-gradient effects. However, these methods do require large computer run times and storage. Another method which is employed in approximate integral or detail boundary-layer codes is mass balancing. The iterative mass-balancing procedure equates the mass flow in the boundary layer at the body point of interest to a streamtube of equal mass in the freestream and requires knowledge of the shock shape and pressure distribution about the blunt body. However, for blunt bodies at incidence, the mass balancing technique presents at best a complex procedure.[50] In addition, in regions of strong vorticity interaction (e.g., turbulent flow in the nose region of blunt bodies) calculated results of turbulent integral and classical boundary-layer analyses employing mass balancing techniques have been shown to overpredict corresponding VSL heat-transfer results by 30-40%.[51]

Considering the inherent difficulties involved with applying mass balancing to three-dimensional flow and the apparent discrepancies resulting from approximate or classical boundary-layer methods for axisymmetric flows, a different approach for approximating variable entropy is used in the study. An inviscid solution is computed, and by means of an iterative process the momentum-thickness and corresponding approximate ratios of boundary-layer thickness to momentum thickness are used to determine the local flow conditions. Thus, this analysis accounts for variable-entropy effects by locally moving out into the inviscid flowfield to a distance equal to the boundary-layer thickness. The inviscid properties at this location are used as the boundary-layer edge properties. Similar concepts for determining variable-entropy edge conditions have been employed in previous investigations.[29,52] It is of interest to note that these studies were based on three-dimensional flow applications.

**Streamline-Spreading Effects**

Analytical[15,27,40] and experimental[17-20] studies have demonstrated that angle of attack has a significant impact on the heating to bodies at incidence especially along the windward ray where heating levels can be an order of magnitude greater than the corresponding leeward rates.[18,19] Obviously, the entire three dimensional viscous flowfield solution[30,31] is preferable if available; however, the computing cost may be prohibitive even for design calculations. A relatively simpler solution is obtained for three-dimensional flows with the axisymmetric analogue.[15] The three-dimensional boundary-layer equations are written in streamline coordinates, and the cross-flow velocity is assumed zero. The resulting equations are identical to the axisymmetric zero AOA forms if the distance along the steamline is considered the surface distance and the metric representing the streamline spreading ($H_2$) is equated to the axisymmetric body radius. This "simpler" technique would still require the solution of the three-dimensional inviscid flowfield[52] or a less rigorous method[15]

of defining a surface streamline path with a computed pressure distribution.

Engineering methods based on the equivalent cone or yawed cylinder approximations have been demonstrated[18,21,22,27] to be unreliable for predicting the shock location and the pressure and heat-transfer levels, especially the laminar heating rates. Thus, there is a need to use satisfactory approximations which account for the effect of the streamline-spreading on the convective heating in engineering procedures. However, such correlations even for axisymmetric bodies are available apparently only for the windward and leeward symmetry planes of sphere-cones.[16,40] The method presented in Ref. 16 is selected for the present analysis and provides at least the flexibility of including the impact of incidence on sphere-cones. The expression for the metric can written as

$$H_2 = (r \cdot a)^{b/c}(\mathrm{d}/a) \tag{3}$$

In the notation of Ref. 16

$$a = (1 + k^2)^{1/2} \tag{4}$$

$$b = k + \tan\alpha\cos\phi \tag{5}$$

$$c = k(1 - k\tan\alpha\cos\phi) \tag{6}$$

and

$$\mathrm{d} = (1 - k\tan\alpha\cos\phi)\cos\alpha \tag{7}$$

where

$$k = \tan\theta_c \tag{8}$$

The term $\cos\phi$ is introduced in this procedure to reduce Eqs. (3-7) to the corresponding forms given for $H_2$ in Ref. 16 for flow in the windward ($\phi = 0$) and leeward ($\phi = 180$) planes. The value $r$ in Eq. (3) is the body cross-sectional radius at an axial location measured along the geometric symmetry line. The leeward-symmetry-plane calculations are restricted to the condition that $\alpha$ is less than $\theta c$. For the corresponding peripheral heating distribution at an axial location, an existing approximation[40] given as

$$q_\alpha/q_{\alpha=0} = (W_q - L_q)\cos(\phi)/2 + (W_q + L_q - 2)\cos(2\phi)/4 + (W_q + L_q + 2)/4 \tag{9}$$

is used in this investigation where $W_q$ represents the ratio of local windward-ray heating at an angle of attack to the respective zero deg AOA value and $L_q$ represents a similar ratio for the leeward ray.

#### Pressure Distributions at $\alpha > 0$

An existing concept[22] based on the extension of the tangent cone method is used herein to model the flowfield along a given meridian of a sphere-cone at incidence. The simulated flow is computed for a blunted cone at zero AOA with an effective half-cone angle given[22] as

$$w = \sin^{-1}(\sin\theta_c\cos\alpha + \cos\theta_c\sin\alpha\cos\phi) \tag{10}$$

The angle $w$ represents the angle between a meridian line and the freestream velocity vector. For the windward plane ($\phi = 0$), $w$ equals $\theta_c + \alpha$; for the leeward plane ($\phi = 180$), $w$ equals $\theta_c - \alpha$. Obviously for $\alpha = 0$, $w = \theta_c$.

As noted, investigations[20,21] which compared experimental shock locations and windward-ray pressures to tangent-cone predictions have shown that the predicted results, (in particular for conditions where the incidence angle is equal to or greater than the cone half-angle) overestimate the measured shock-layer thickness and pressure levels downstream of the shock inflection point. However, at measuring stations upstream of the shock-inflection point the surface pressure measurements and predicted results are in very good agreement.[22]

In the present code, the shock angle downstream of the minimum inflection point approaches a shock angle value given by

$$\theta_{sc} = \sin^{-1}[(1/M_\infty^2) + (\gamma + 1)\sin^2 w/2] \tag{11}$$

for sphere-cones at zero AOA. The effective cone angle $w$ defined by Eq. (10) is modified for use in Eq. (11) as

$$w = 0.95(w - \theta_c) + \theta_c \tag{12}$$

The results of substituting Eq. (12) in Eq. (11) produce a lower value of $\theta_{sc}$, and thus shock-layer thickness on the windward side and the opposite trend in the leeward plane.

## Results and Discussion

In this section, predicted results which demonstrate the additional capabilities of the present engineering code are compared with surface measurements on sphere-cones at several AOA conditions, including incidence angles greater than the cone half-angle. The importance of incorporating an approximation to the metric defining streamline spreading in heating calculations for sphere-cones at incidence is demonstrated by comparison with predictions using only the equivalent-cone concept. This present engineering method is limited to conditions for which the sonic line remains on the spherical nose and to leeward ray applications where the angle of attack is less than the half-cone angle.

Before discussing the current results, previous applications of the method are noteworthy. The present code has been validated by comparison with the data and detailed predictions used to establish the original engineering code. For example, in Ref. 51, calculated results or turbulent integral and detailed boundary-layer analyses employing mass-balancing techniques were shown to overpredict corresponding VSL results by 30-40%. However, calculated results of the original[34] and present engineering codes yield discrepancies of generally less than 15% when compared to VSL results. Also a point of interest, the present engineering method required approximately 35 s on the CDC 6600 computer, while the corresponding VSL solution requied 240 s. A boundary-layer mass balancing procedure,[26] which includes the tangential velocity normal to the surface as a boundary condition, required approximately 150 s. Experimental results for shock shapes and pressure and heat-transfer distributions over hyperboloids, paraboloids, and 45-deg half-angle spherically blunted cones at zero AOA were compared[23] to corresponding calculated results based on the present procedure and very good comparisons were noted. Also, the heating equations and equilibrium-air correlations,[53] which can be used in the present method, have been incorporated in an axisymmetric analogue method. The resulting heating-rate calculations were compared with perfect gas and equilibrium heating based on heating options in the code. As a result of those investigations,[54,55] the present equilibrium-air correlations have been selected as the basis of calculation in the axisymmetric analogue code. The results of the heating calculations using the methods described herein were found to yield at least an equally good a comparison. However, note that the present method produces also the detailed distribution of the flowfield properties including the inviscid surface pressure distribution.

In Figs. 1-3, comparisons of the computed and experimental pressure distributions are noted to be in good agreement. The experimental[56] and calculated windward-ray pressure distribution on a 7-deg half-angle blunt cone at 10 deg angle of attack and a freestream Mach number of 8.0 is

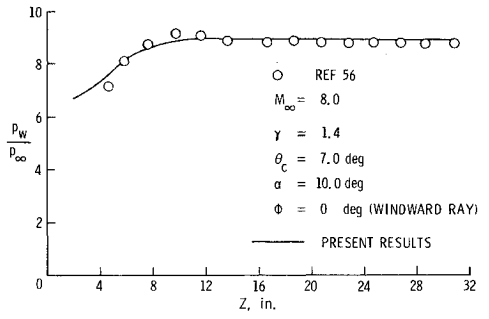


**Fig. 1 Comparison of predicted and measured surface pressures.**

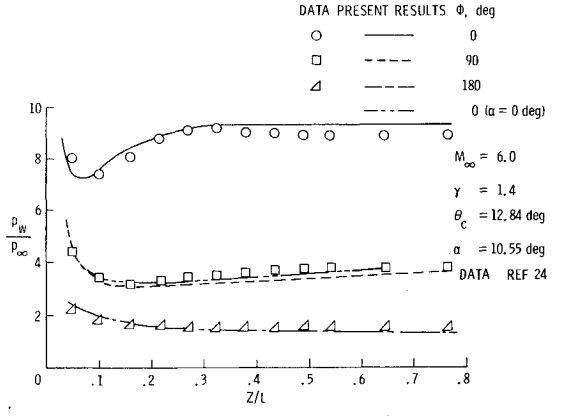


**Fig. 2 Comparison of predicted and measured surface pressures.**

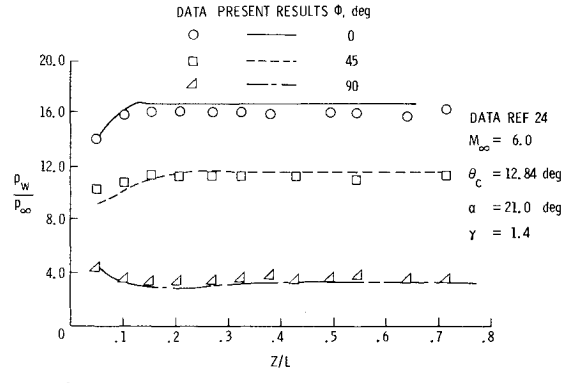


**Fig. 3 Comparison of predicted and measured surface pressures.**

presented in Fig. 1. Selected experimental[24] and computed meridional pressure distributions on a 12.84 deg blunt cone at a freestream Mach number of 6.0 are presented in Figs. 2 and 3 at angles of attack of 10.55 deg and 21.0 deg, respectively. In Fig. 2 the experimental and predicted pressure distributions at $\phi = 90$ deg are compared with corresponding predicted results at zero AOA. Discrepancies of less than 10% are noted. These comparisons are typical of conclusions in existing investigations.[17,18] The data and predicted values are present only to $\phi = 90$ in Fig. 3, since a pressure minimum was observed in the circumferential experimental data at $\phi = 135$ deg. This occurrence of a pressure minimum other than at the leeward ray is indicative of flow separation.

Heat-transfer comparisons are present in Figs. 4 and 5. In Fig. 4 the predicted and measured[19] heating data for a 15-deg blunt cone at a freestream Mach number of 10.6 and angles of attack of 0, 10, and 20 degs are presented. For both 10 and 20 deg AOA, experimental data are presented along the 0 and 90 deg circumferential locations and also along the leeward ray for 10 deg AOA. At angles of attack of 0, 5, 10, and 15 deg,

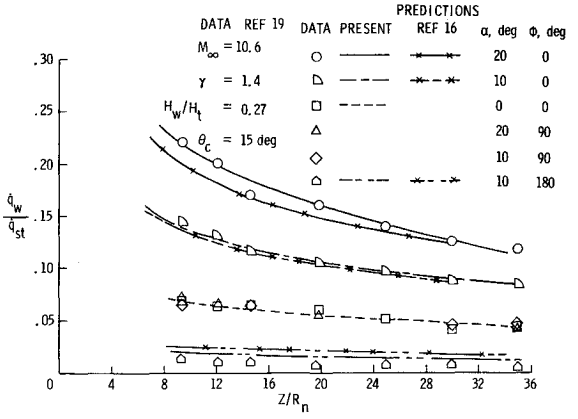


**Fig. 4 Comparison of predicted and measured heating rates.**

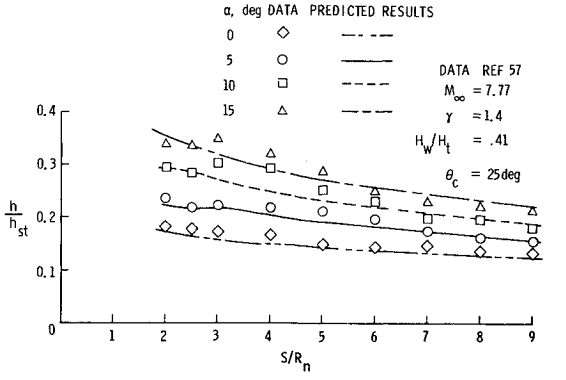


**Fig. 5 Comparison of predicted and measured windward-ray heating rates.**

experimental[57] and calculated windward-ray heat-transfer data for a 25-deg blunt cone at a freestream Mach number of 7.77 are compared in Fig. 5. For zero AOA, and for the windward-ray conditons at angle of attack, the comparisons of the experimental data with the calculated results shown in Figs. 4 and 5 are good, with discrepancies typically less than 5% and maximum values less than approximately 10%. However, the experimental leeward-ray data level presented in Fig. 4 is approximately 50% of the present predicted results. Similar discrepancies along the leeward ray are noted for heating rates measured on the 15-deg blunt cone at a 5 deg AOA condition (not presented herein). Fortunately, the windward heating rates on these rather slender cones are as much as a factor of ten greater than the corresponding leeward rates, and thus the leeward rates are not critical to the thermal design. For larger half-cone angles and similar incidence levels (see Ref. 57 at 5-deg and 10-deg AOA), predicted heating rates based on the present method more adequately describe the experimental leeward heating levels (within 20%). Note that the present calculated heating distributions are in better agreement ($\approx 10\%$) with the data presented in Fig. 4 than the calculated rates based on the approximate code[16] using the axisymmetric analogue. The calculation technique of Ref. 16 is based on a Newtonian pressure distribution which may be a partial explanation for the differences. The experimental leeward-ray data level is about one third of the predicted values of Ref. 16. In Fig. 4, experimental data for zero AOA and for 10 and 20 deg AOA along the 90 deg meridian are compared with predicted zero angle of attack values. The heating rates calculated for zero AOA are shown to represent the experimental heating distribution for both AOA conditions along the 90 deg meridional plane adequately. Thus, for the conditions considered herein, the effect of angle of attack on the heating as

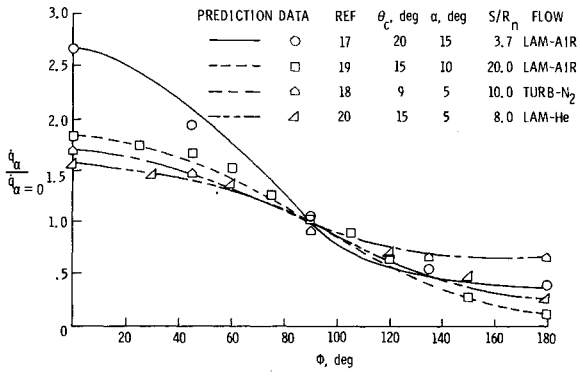


**Fig. 6 Comparison of predicted and measured circumferential heating rates.**

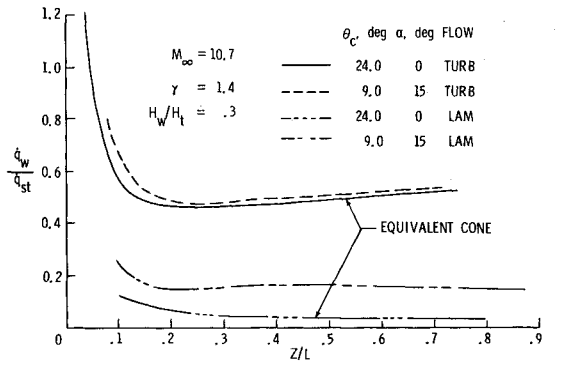


**Fig. 7 Angle of attack effects on laminar and turbulent heating rates.**

well as the pressure distributions along the 90-deg meridian appears to be insignificant. Similar conclusions have been reported[17,18] for $\alpha/\theta_c < 2.0$.

The technique to account for the effect of streamline spreading on the heat transfer is applicable only to sphere-cone windward or leeward symmetry planes. The empirical relation[40] given by Eq. (9) can be used to determine required circumferential heating distributions. Experimental circumferential heating distributions are compared in Fig. 6 with approximate results calculated with Eq. (9). The flow conditions represent laminar and turbulent flow in a test median of air, nitrogen, or helium. The data are representative of conditions with the angle of attack less than the body half-angle for which flow separation is not apparent. The predicted values using the experimental windward and leeward rates are shown to be in good agreement with the circumferential experimental data. Similar comparisons are noted to approximately $\phi = 90$ deg when flow separation occurs (results not presented in this paper). Note that calculated windward and leeward heating rates resulted in equally good comparisons with the experimental data to approximately the $\phi = 150$-deg circumferential body location. These experimental leeward rates have been noted to be approximately one-half the predicted rates.

The significance of including the present approximation to the metric for streamline spreading in the engineering heating calculation is demonstrated in Fig. 7. Laminar and turbulent heating rates using the approximation for the streamline spreading metric are compared to corresponding results based on the equivalent cone method. The predicted laminar heating rates using the streamline-spreading approximation are shown to be significantly larger than calculated values based on the equilvalent cone method. The turbulent heating levels based on either including the metric approximations or using only the equivalent cone technique are shown to be in much better agreement. This comparison demonstrates only the capability of the present method to reproduce results which have been reported in the literature.[18,27] Adams[27] reported that such results should be expected based on an analysis of Vaglio-Laurin.[10] Due to large turbulent shearing stress, smaller three-dimensional effects are computed for turbulent conditions than for comparable laminar conditions.

## Conclusions

The applicability of an engineering inviscid flowfield method has been extended to include heat-transfer predictions applicable to perfect gas or equilibrium chemistry at conditions of constant or variable-entropy. The variable-entropy effects on the heat transfer are approximated by defining the local edge properties as the inviscid values located a distance from the body equal to the boundary-layer thickness. The approximate code computes the inviscid flowfield over hyperboloids, ellipsoids, paraboloids, and blunt or slender sphere cones at zero-deg angle of attack. An application to angle-of-attack conditions is included in this engineering method by incorporating existing approximations to account for the streamline spreading impact on the calculated sphere-cone windward or leeward ray heat transfer and to account for the corresponding circumferential heating distributions. Pressure distributions can be computed along any arbitrary meridian ray provided boundary-layer separation has not occurred.

Predicted pressure and heat-transfer distributions are compared with corresponding experimental data over an angle-of-attack range including incidence angles greater than the body half-angle. Discrepancies of generally less than 10% are obtained, except for leeward heating-rate comparisons. The pressure and heat-transfer data along the 90 deg meridian are observed to be essentially independent of angle of attack and predicted by the zero angle of attack calculated results. Circumferential experimental heat-transfer data are shown to be adequately predicted by the approximate expression. The equivalent-cone method is illustrated to be unreliable in predicting laminar heating rates but produces satisfactory turbulent heating levels.

The engineering code provides a rapid yet reliable method for defining surface-measurable quantities such as pressure and heat transfer, and also flow properties throughout the shock layer. The later capability is not available in usual engineering heating methods. The present method represents a versatile method for parametric or preliminary thermal design studies.

## References

[1] Fay, J.A. and Riddell, F.R., "Theory of Stagnation-Point Heat Transfer in Dissociated Air," *Journal of Aerospace Sciences*, Vol. 25, No. 2, Feb. 1958, pp. 73-85, 121.

[2] Cohen, N.B., "Boundary-Layer Similar Solutions and Correlation Equations for Laminar Heat-Transfer Distribution in Equilibrium Air at Velocities Up to 41,000 Feet Per Second," NASA TR R-118, 1961.

[3] Kemp, N.H., Rose, P.H., and Detra, R.W., "Laminar Heat Transfer Around Blunt Bodies in Dissociated Air," *Journal of Aerospace Sciences*, Vol. 26, No.7, July 1959, pp. 421-430.

[4] Zoby, E.V., "Approximate Relations for Laminar Heat Transfer and Shear Stress Functions in Equilibrium Dissociated Air," NASA TN D-4484, April 1968.

[5] Sutton, K. and Graves, R.A., Jr., "A General Stagnation Point Convective Heating Equation for Arbitrary Gas Mixtures," NASA TR R-376, Nov. 1971.

[6] Marvin, J.G. and Deiwert, G.S. "Convection Heat Transfer in Planetary Gases," NASA TR R - 224, July 1965.

[7] Zoby, E.V. and Graves, R.A. Jr., "Comparison of Results from Three Prediction Methods with Turbulent-Heating Data Wind Tunnel and Free Flight Test," NASA TM X-2390, Sept. 1971.

[8] Libby, P.A. and Cresci, R.J., "Evaluation of Several Hypersonic Turbulent Heat Transfer Analyses by Comparison with Experimental Data," WADC TN 57-72, July 1957.

[9] Phillips, R.L., "A Summary of Several Techniques Used in the Analysis of High Enthalpy Level, High Cooling Ratio Turbulent

Boundary Layers of Blunt Bodies of Revolution," GM-TM-194, Ramo Wooldridge Corp., Sept. 1957.

[10]Vaglio-Laurin, R., "Turbulent Heat Transfer on Blunt Nosed Bodies in Two-Dimensional Hypersonic Flow," *Journal of Aerospace Sciences,* Vol. 27, No. 1, Jan. 1960, pp. 27-36

[11]Cresci, R.J., MacKenzie, D.A., and Libby, P.A. "An Investigation of Laminar, Transitional, and Turbulent Heat Transfer on Blunt-Nosed Bodies in Hypersonic Flow," *Journal of Aerospace Sciences,* Vol. 27, No.6, June 1960, pp. 401-414.

[12]Johnson, C.B. and Boney, L.R., "A Simple Integral Method for the Calculation of Real-Gas Turbulent Boundary Layers with Variable Edge Entropy," NASA TN D-6217, June 1971.

[13]Vaglio-Laurin, R., "Laminar Heat Transfer on Three-Dimensional Blunt Nosed Bodies In Hypersonic Flows," *American Rocket Society Journal,* Vol. 29, No. 2, Feb. 1959, pp. 123-129.

[14]Hecht, A.M. and Nestler, D.E., "A Three-Dimensional Boundary-Layer Computer Program for Sphere-Cone Type Re-Entry Vehicles," Vol. 1, *Engineering Analysis and Code Description,* AFFDL-TR-78-67, June 1978.

[15]DeJarnette, F.R. and Hamilton, H.H., "Aerodynamic Heating on 3 – D Bodies Including the Effects of Entropy-Layer Swallowing," *Journal of Spacecraft and Rockets,* Vol. 12, Jan. 1975, pp. 5-12.

[16]DeJarnette, F.R. and Davis, R.M. "A Simplified Method for Calculating Laminar Heat Transfer Over Bodies at an Angle of Attack," NASA TN-4720, 1968.

[17]Zakkay, V., "Pressure and Laminar Heat Transfer Results in Three-Dimensional Hypersonic Flow," WADC TN 58-182, Sept. 1958.

[18]Widhopf, G.F., "Turbulent Heat-Transfer Measurements on a Blunt Cone at Angle of Attack," *AIAA Journal,* Vol. 9, Aug. 1971, pp. 1574-1580.

[19]Cleary, J.W., "Effects of Angle of Attack and Bluntness on Laminar Heating-Rate Distributions on a 15° Cone at a Mach Number of 10.6," NASA TN D – 5450, Oct. 1969.

[20]Cleary, J.W. and Duller, C.E., "Effects of Angle of Attack and Bluntness on the Hypersonic Flow Over a 15° Semiapex Cone in Helium," NASA TN D-5903, Aug. 1970.

[21]Cleary, J.W., "Effects of Angle of Attack and Bluntness on the Shock- Layer Properties of a 15° Cone at a Mach Number of 10.6," NASA TN D-4909, Nov. 1968.

[22]Cleary, J.W., "An Experimental and Theoretical Investigation of the Pressure Distribution and Flow Fields of Blunted Cones at Hypersonic Mach Numbers," NASA TN D-2969, Aug. 1965.

[23]Miller, C. G., "Measured Pressure Distributions, Aerodynamic Coefficients, and Shock Shapes on Blunt Bodies at Incidence in Hypersonic Air and $CF_4$," NASA TM 84489, Sept. 1982.

[24]Miller, C.G. and Gnoffo, P.A., "An Experimental Investigation of Hypersonic Flow Over Biconics at Incidence and Comparison to Prediction," AIAA Paper 82-1382, Aug. 1982.

[25]Lin, T.C., Rubin, S.G., and Widhopf, G.F., "A Two-Layer Model for Coupled Three Dimensional Viscous and Inviscid Flow Calculations," AIAA Paper 81-0118, Jan. 1981.

[26]Anderson, E.C. and Wilcox, D.C., "Transitional Boundary-Layer Solutions Using a Mixing-Length and a Two-Equation Turbulence Model," NASA CR-2986, April 1978.

[27]Adams, J.C., Jr., "Implicit Finite-Difference Analysis of Compressible Laminar, Transitional, and Turbulent Boundary Layers Along the Windward Streamline on a Sharp Cone at Incidence," AEDC-TR-71-235, Dec. 1971.

[28]Stainback, P.C. (with Appendix by P.C. Stainback and K.C. Wicker) "Effect of Unit Reynolds Number, Nose Bluntness, Angle of Attack, and Roughness on Transition on a 5° Half-Angle Cone at Mach 8," NASA TN D-4961, 1969.

[29]Propinski, Z. "Compressible Laminar Boundary Layers on Sharp Cones at Incidence with Entropy Swallowing," *AIAA Journal,* Vol. 13, Sept. 1975, pp. 1135-1136.

[30]Helliwell, W.S., Dickinson, R.P., and Lubard, S.C., "Viscous Flow Over Arbitrary Geometries at High Angle of Attack," *AIAA Journal,* Vol. 19, Feb. 1981, pp. 191-197.

[31]Gnoffo, P.A., "Hypersonic Flows Over Biconics Using a Variable-Effective Gamma, Parabolized-Navier-Stokes Code," AIAA Paper 83-1666, July 1983.

[32]Mayne, A.W., Jr., "Calculation of the Laminar Viscous Shock Layer on a Blunt Body at Incidence to Supersonic and Hypersonic Flow," AEDC-TR-76-123, Dec. 1976.

[33]Moss, J.N., "Stagnation and Downstream Viscous Shock Layer Solutions with Radiation and Coupled Ablation Injection," AIAA Paper 74-73, Jan. 1974.

[34]Zoby, E.V., Moss, J.N., and Sutton, K., "Approximate Convective Heating Equations for Hypersonic Flows," *Journal of Spacecraft and Rockets,* Vol. 18, Jan. 1981, pp. 64-70.

[35]Sutton, K., "Characteristics of Coupled Nongray Radiating Gas Flows with Ablation Product Effects About Blunt Bodies During Planetary Entries," Ph.D Thesis, North Carolina State University, Raleigh, N.C., 1973.

[36]Falanga, R.A. and Olstad, W.B., "An Approximate Inviscid Radiating Flow-Field Analysis for Sphere-Cone Venusian Entry Vehicles," AIAA Paper 76-758, 1974.

[37]Zoby. E.V., "Approximate Heating Analysis for the Windward Symmetry Plane of Shuttle-like Bodies at Large Angle of Attack," *Progress in Astronautics and Aeronatics: Thermophysics of Atmospheric Entry,* Vol. 82, T.E. Horton, ed., AIAA, New York, 1981, pp. 229-247.

[38]Zoby, E.V., "Analysis of STS-2 Experimental Heating Rates and Transition Data," *Journal of Spacecraft and Rockets,* Vol. 20, May-June 1983, pp. 232-237.

[39]Zoby, E.V. and Graves, R.A., Jr., "A Computer Program for Calculating the Perfect Gas Inviscid Flow Field About Blunt Axisymmetric Bodies at an Angle of Attack of 0°," NASA TM X-2843, Dec. 1973.

[40]Heins, A.E. and Estes, T.J., "Effects of Angle of Attack on Laminar Convective Heat Transfer on Sharp and Blunt Cones," TIS 61SD70, General Electric, April 1961.

[41]Maslen, S.H., "Inviscid Hypersonic Flow Past Smooth Symmetric Bodies," *AIAA Journal,* Vol. 2, June 1964, pp. 1055-1061.

[42]Maslen, S.H., "Axisymmetric Hypersonic Flow," NASA CR-2123, 1972.

[43]Jackson, S.K., Jr., "The Viscous-Inviscid Hypersonic Flow of a Perfect Gas Over Smooth Symmetric Bodies," Ph.D Thesis, University of Colorado, Boulder, Colo., 1966.

[44]Spalding, D.B. and Chi, S.W., "The Drag of a Compressible Turbulent Boundary Layer on a Smooth Flat Plate With and Without Heat Transfer," *Journal of Fluid Mechanics,* Vol. 18, Pt. 1, Jan. 1964, pp. 117-143.

[45]Cary, A.M., Jr. and Bertram, M.H., "Engineering Predictions of Turbulent Skin Friction and Heat Transfer in High Speed Flow," NASA TN D-7507, 1974.

[46]White, F.M., *Viscous Fluid Flow,* McGraw-Hill, New York, 1974.

[47]Kutateladze, S.S. and Leont'ev, A.I., *Turbulent Boundary Layers in Compressible Gases,* Academic Press, Inc., New York, 1964.

[48]Johnson, C.B. and Bushnell, D.M., "Power-Law Velocity-Profile-Exponent Variations With Reynolds Number, Wall Cooling, and Mach Number in a Turbulent Boundary Layer," NASA TN D-5753, April 1970.

[49]Ferri, A., "Some Heat-Transfer Problems in Hypersonic Flow," *Aeronautics and Astronautics,* Pergamon Press, New York, 1960, pp. 344-377.

[50]Mayne, A.W., Jr., "Calculation of the Boundary Layer Flow in the Windward Symmetry Plane of a Spherically Blunted Axisymmetric Body at Angle of Attack, Including Streamline-Swallowing Effects," AEDC-TR-73-166, Oct. 1973.

[51]Anderson, E.C., Moss, J.N., and Sutton, K., "Turbulent Viscous-Shock-Layer Solutions with Strong Vorticity Interaction," *Journal of Spacecraft and Rockets,* Vol. 14, Jan. 1977, pp. 32-37.

[52]Goodrich, W.D., Li, C.P., Houston, C.K., Chiu, P.B., and Olmedo, L., "Numerical Computations of Orbiter Flowfields and Laminar Heating Rates," *Journal of Spacecraft and Rockets,* Vol. 14, May 1977, pp. 257- 264.

[53]Zoby, E.V., and Moss, J.N., "Thermodynamic Equilibrium-Air Correlations for Flowfield Applicaiotn," *AIAA Journal,* Vol. 20, June 1982, pp. 849-854.

[54]Chitty, A., "A Computational Method for Approximate Predictions of Convective Aerodynamic Heating Rates on Prescribed Geometries in Hypersonic Flows," Master Thesis, Department of Mechanical and Aerospace Engineering, North Carolina State University, Raleigh, N.C., 1981.

[55]DeJarnette, F.R., Kania, L.A., and Chitty, A., "Aerodynamic Heating and Surface Temperatures on Vehicles for Computer-Aided Design Studies," AIAA Paper 83-0411, Jan. 1983.

[56]Harris, T.B., "An Efficient Method for Supersonic Viscous Flow Field Calculations," AIAA Paper 83-0222, Jan. 1983.

[57]Bushnell, D.M., Jones, R.A. and Huffman, J.K., "Heat-Transfer and Pressure Distributions on Spherically-Blunted 25° Half-Angle Cone at Mach 8 and Angles of Attack up to 90°," NASA TN D – 4792, Oct. 1968.